fishes

MDPI

Article

Integrated Transcriptome and Metabolome Analysis Elucidates the Effects of Three Dietary Additives on Growth and Antioxidant Function in Juvenile *Rhinogobio ventralis*

Wen Chen [1,2,†], Zhenni Wu [2,†], Lin Luo [1], Min Guan [1], Xiaojuan Cao [2] and Jian Gao [2,*]

[1] Hubei Key Laboratory of Three Gorges Project for Fish Resource Conservation (Chinese Sturgeon Research Institute of China Three Gorges Corporation), Yichang 443100, China
[2] College of Fisheries, Engineering Research Center of Green Development for Conventional Aquatic Biological Industry in the Yangtze River Economic Belt, Ministry of Education, Huazhong Agricultural University, Wuhan 430070, China
* Correspondence: gaojian@mail.hzau.edu.cn
† These authors contributed equally to this work.

Abstract

An 8-week feeding trial was conducted to investigate the regulatory effects of dietary chitosan oligosaccharide (COS), chlorogenic acid (CGA), and thymopeptide (TH) on the growth performance, antioxidant capacity, and metabolism of juvenile *Rhinogobio ventralis*. A control group (CON) and three treatment groups (COS, CGA, TH) were established, and the underlying molecular mechanisms were analyzed by transcriptomics and metabolomics. The results showed that dietary supplementation with COS, CGA, and TH significantly improved weight gain rate, specific growth rate, and feed utilization efficiency, with COS exhibiting the strongest growth-promoting effect. COS also significantly increased hepatic catalase and superoxide dismutase activities and decreased malondialdehyde content, indicating a marked antioxidant effect, whereas CGA and TH showed no significant effects on these parameters. Transcriptomic analysis revealed significant differences in gene expression profiles among the groups, with commonly enriched pathways including the FoxO signaling pathway, fatty acid biosynthesis, and nicotinate and nicotinamide metabolism. Metabolomic analysis showed that the three additives significantly reshaped the hepatic metabolic profiles: COS mainly activated anabolic metabolism, CGA predominantly suppressed metabolism, and TH exhibited bidirectional regulation, with bile secretion, neuroactive ligand–receptor interaction, and the Fc epsilon RI signaling pathway commonly enriched in all three groups. Integrative KEGG pathway analysis based on transcriptomic and metabolomic predictions further identified the FoxO signaling pathway and neuroactive ligand–receptor interaction as common targets shared by all three additives. In conclusion, COS, CGA, and TH improve the health status of *R. ventralis* through differential regulation of immune–metabolic networks. Among them, COS is the most suitable feed additive for growth promotion and antioxidant protection in this species.

Keywords: *Rhinogobio ventralis*; chitosan oligosaccharide; chlorogenic acid; thymopeptide; growth performance; antioxidant capacity; transcriptome; metabolome

Key Contribution: This is the first systematic study comparing COS, CGA, and TH in juvenile *Rhinogobio ventralis*. COS best improved growth and antioxidant capacity. Multi-omics revealed FoxO signaling and neuroactive ligand–receptor interaction as core pathways, supporting functional feed development for this endangered fish.

Academic Editor: Qiyou Xu

Received: 18 May 2026
Revised: 25 June 2026
Accepted: 26 June 2026
Published: 3 July 2026

1. Introduction

Rhinogobio ventralis is distributed in the mainstream and tributaries of the Jinsha River within the upper and middle reaches of the Yangtze River in China. As an endemic fish species to the Jinsha River basin, it is Listed as National Class II Key Protected Wild Animal in China [1]. In recent years, owing to a combination of factors including overfishing, habitat degradation, and water pollution, the population of *R. ventralis* has undergone a substantial decline, resulting in a pronounced reduction in its wild stock resources. Concurrently, with advancements in artificial propagation techniques, artificial enhancement and release have emerged as an important strategy for the restoration of its population resources. Nevertheless, juveniles obtained through artificial incubation exhibit marked sensitivity to the aquaculture environment. Fluctuations in various physicochemical parameters of the water environment, as well as the presence of environmental organisms—particularly *Ichthyophthirius multifiliis* and various bacterial pathogens—readily induce stress responses in these juveniles, leading to frequent disease outbreaks and subsequent mortality [2,3]. Consequently, the development of functional feed additives capable of enhancing growth performance, improving immune function, and augmenting stress resistance is fundamental to achieving large-scale artificial enhancement and release of *R. ventralis*.

To address these challenges, the inclusion of functional feed additives has emerged as an important strategy to enhance the intrinsic disease resistance and stress tolerance of juvenile fish. Among these, immunostimulants are considered a promising approach for ensuring aquatic animal health and promoting green aquaculture practices, as they can activate the non-specific immune system, improve antioxidant enzyme activities, and mitigate pathogen-induced damage without inducing drug resistance.

Despite their low inclusion levels in aquafeeds, immunostimulants play disproportionately critical roles in activating non-specific immune defenses and mitigating oxidative stress induced by environmental and pathogenic challenges [4–6]. Chitosan oligosaccharide (COS), a depolymerized product of chitosan derived from crustacean shells, exhibits excellent water solubility and biodegradability, and has been demonstrated, when supplementing 0.5–2%, to possess multiple biological activities, including immunomodulation, antioxidant effects, and antibacterial properties, in *Oreochromis niloticus* and *Pelodiscus sinensis* [7–9]. Chlorogenic acid (CGA) is a natural phenolic compound found in various plants, such as *Eucommia ulmoides* and *Lonicera japonica*, and has shown significant antioxidant, anti-inflammatory, and antibacterial activities in studies on *Cyprinus carpio* and *Protonibea diacanthus* [10,11]. Thymopeptide (TH) is a polypeptide hormone derived from thymic tissue, known for its ability to promote T-lymphocyte differentiation and maturation, thereby enhancing cellular immune responses [12,13]. Although COS, CGA, and TH each possess respective merits as feed additives, existing research has predominantly focused on their individual effects in a limited number of economically important aquaculture species, such as *C. carpio*, *O. niloticus*, and *P. sinensis*. To the best of our knowledge, no published study has systematically evaluated or compared the effects of dietary supplementation with COS, CGA or TH on growth performance, antioxidant capacity, immune responses, and metabolism in *R. ventralis*. Furthermore, it remains unclear whether these three compounds exert distinct or comparable modulatory effects on the physiological and metabolic status of this endangered fish species.

In recent years, transcriptomics and metabolomics have emerged as important tools for studying nutrition and growth in aquatic animals. Transcriptomics provides a deeper understanding of how different nutrients, feed formulations, and environmental factors influence gene expression. Previous studies have employed transcriptomic analysis to elucidate the immunomodulatory mechanisms of feed additives. For instance, Núñez-Acuña et al. [14] evaluated the transcriptomic response of *Salmo salar* fed with plant-derived

in-feed additives following *Caligus rogercresseyi* infestation, revealing that immune response genes were the most variable, particularly in the head kidney, while metabolic genes were highly expressed in individuals fed with immunostimulant-supplemented diets. Similarly, Chen et al. [15] demonstrated through transcriptome analysis that *Salvia miltiorrhiza* polysaccharide (SMP) supplementation enhanced cellular and humoral immunity in *Procambarus clarkii* by up-regulating genes involved in lysosome, phagosome, and endocytosis signaling pathways. On the other hand, metabolomics offers complementary information by profiling the metabolites involved in cellular processes, such as amino acids, lipids, and carbohydrates, revealing how dietary modifications affect the metabolism of aquatic animals. Natnan et al. [16] employed metabolomic profiling to investigate the effects of oleic acid as an immunostimulant in hybrid grouper (*Epinephelus fuscoguttatus* × *E. lanceolatus*) challenged with *Vibrio vulnificus*, identifying glycine, serine, and threonine metabolism as the most impacted pathways in the spleen and liver. Furthermore, integrated multi-omics approaches have been applied to investigate the effects of nutritional enhancers. Jia et al. [17] combined transcriptomic and metabolomic analyses to demonstrate that dietary proanthocyanidins improved antioxidant capacity, muscle nutrients, and intestinal microbiota diversity in *C. carpio*, with the regulation of lipid metabolism linked to changes in the PPAR signaling pathway and intestinal microbiota composition. These approaches collectively provide a deeper understanding of how nutritional enhancers influence gene expression and metabolism in aquatic organisms, thereby advancing our knowledge of aquatic nutrition and facilitating the development of more sustainable and efficient feeding strategies in aquaculture.

Therefore, the present study aims to investigate the physiological, molecular, and metabolic responses of juvenile *R. ventralis* to dietary supplementation with chitosan oligosaccharide, chlorogenic acid, and thymosin administered separately. The assessment parameters encompass growth performance, antioxidant capacity, transcriptomic profiling, and metabolomic analysis. The primary objective of this study is to provide a scientific basis for the development of targeted, effective, and safe functional feed formulations for juvenile *R. ventralis* used in artificial enhancement and release programs, thereby establishing a research foundation for both the conservation of this species and its large-scale artificial enhancement and release.

2. Materials and Methods

2.1. Diet Preparation and Dietary Treatments

For the experimental trial, four isonitrogenous and isolipidic experimental diets were formulated to evaluate the effects of different nutritional enhancers on *R. ventralis*. The four diets were designated as follows: a control diet containing no nutritional enhancer supplementation (CON), a diet supplemented with COS, a diet supplemented with CGA, and a diet supplemented with TH. The formulation of the four diets is presented in Table 1.

Chitosan oligosaccharide (purity $\geq$ 99%) was purchased from Huatai Biotechnology Co., Ltd. (Xinxiang, China). Chlorogenic acid (purity $\geq$ 70%) was obtained from Peiwei Biological Raw Materials Co., Ltd. (Xi'an, China). Thymosin (purity $\geq$ 99%) was also purchased from Peiwei Biological Raw Materials Co., Ltd. (Xi'an, China). All dietary ingredients were thoroughly mixed, and distilled water was added to achieve an appropriate consistency. The mixture was then pelleted using a laboratory feed extruder, and the pellets were extruded into a diameter of 2 mm. After the feed was thoroughly crushed, it was sieved through a 30–60 mesh screen to obtain pellet particles of 0.2 mm. The pellets were immediately dried at 25 °C to reduce the moisture content and subsequently stored at −20 °C until further use.

Table 1. Ingredient of the experimental diets (%, DM basis).

	Experimental Diets			
	Con	**COS**	**CGA**	**TH**
Fish Meal [1]	50.0	50.0	50.0	50.0
Whey Protein Powder	10.0	10.0	10.0	10.0
Shrimp Meal	10.0	10.0	10.0	10.0
Soy Protein Isolate [2]	6.0	6.0	6.0	6.0
Vitamin-Mineral Premix [3]	3.0	3.0	3.0	3.0
Phospholipid Oil [4]	4.0	4.0	4.0	4.0
Chitooligosaccharide [5]	-	0.5	0.0	0.0
Chlorogenic Acid [6]	-	-	0.5	-
Thymosin [7]	-	-	-	0.5
Sodium Alginate [8]	1.0	1.0	1.0	1.0
a-Starch [9]	8.0	8.0	8.0	8.0
CMC [10]	8.0	7.5	7.5	7.5

[1] Fish meal: Pequera Diamante, Lima, Peru, [2] Soy protein isolate: Anyang Tianrui Food Technology Co., Ltd., Anyang, China. [3] Vitamin and mineral premix: Liankui Feed Additives Co., Ltd., Jinan, China. [4] Soybean phospholipid oil: Zhongchuang Feed Additive Co., Ltd., Binzhou, China. [5] Chitooligosaccharide: Peptide Biotechnology Co., Ltd., Hangzhou, China. [6] Chlorogenic acid: Peptide Biotechnology Co., Ltd., Hangzhou, China. [7] Thymosin: Peptide Biotechnology Co., Ltd., Hangzhou, China. [8] Sodium alginate: Sinopharm Chemical Reagent Co., Ltd., Shanghai, China. [9] α-starch: Jiahe Xuri Company, Linyi, China. [10] Carboxymethyl cellulose (CMC): Sinopharm Chemical Reagent Co., Ltd., Shanghai, China.

2.2. Experimental Design and Feeding Management

The eight-week experiment was conducted at the Rare and Endemic Fish Breeding and Release Station of the Wudongde Hydropower Station in the Jinsha River, China, utilizing a recirculating aquaculture system. Artificially bred juvenile *R. ventralis* at one month of age were selected for the experiment, all originating from the same batch of artificially reproduced wild F1 population. Prior to the start of the experiment, the juveniles were fasted for 24 h. Subsequently, 120 juveniles were randomly selected from this population, collectively weighed, and then randomly and equally divided into 3 groups of 40 fish each. A total of 12 groups of juvenile *R. ventralis* were collectively weighed and then randomly distributed into 12 rearing tanks (each tank measuring 2 m in diameter and 1 m in water depth). Each dietary treatment group was assigned three replicate tanks.

During the 56-day (equivalent to eight weeks) experimental period, the juveniles were fed twice daily at 07:00 and 17:30. The daily feeding rate was maintained at 1% of the juvenile's body weight. To maintain water quality and dissolved oxygen levels, the entire rearing system was connected to a recirculating aquaculture system. During the experimental period, water quality parameters including dissolved oxygen and temperature were monitored and remained within normal ranges.

2.3. Sample Collection

At the conclusion of the experiment, juvenile *R. ventralis* were fasted for an additional 24 h. Thereafter, all individuals in each rearing tank were carefully collected, weighed, and counted. Ten fish were randomly selected from each rearing tank for the measurement of body weight and body length. Liver samples were collected from three juvenile *R. ventralis* from each rearing tank, immediately frozen in liquid nitrogen, and stored at −80 °C for subsequent analyses. Additionally, three liver samples per treatment group were collected for transcriptomic analysis. For metabolomic analysis, three liver samples were collected from different experimental juveniles across the three replicate tanks within each treatment group to account for biological variability and enhance the reliability of the non-targeted metabolomics data.

2.4. Biochemical Analysis

The activities of antioxidant enzymes and the level of lipid peroxidation products were quantitatively determined in the liver samples of *R. ventralis*. Specifically, the activities of superoxide dismutase (SOD) and catalase (CAT), as well as the malondialdehyde (MDA) content, were measured in liver homogenates. All assays were performed using commercial reagent kits following the manufacturer's instructions. The kits were purchased from Nanjing Jiancheng Bioengineering Institute (Nanjing, China). Each sample was analyzed in triplicate to ensure the accuracy and reproducibility of the results. The enzyme activities and MDA levels were normalized to the total protein content of the liver homogenates, which was determined using the bicinchoninic acid (BCA) method.

2.5. Transcriptomics Analysis

Total RNA was extracted from the liver samples of juvenile *R. ventralis* using TRIzol® Reagent. RNA quality was assessed using an Agilent 5300 bioanalyzer (Thermo Fisher Scientific, Waltham, MA USA) and quantified with a NanoDrop ND-2000 spectrophotometer (Thermo Fisher Scientific, Waltham MA). Only high-quality RNA samples (OD260/280 = 1.8–2.2, RQN $\geq$ 6.5, >1 μg) were used for library construction.

RNA-seq libraries were prepared using the Illumina® Stranded mRNA Prep Kit following the manufacturer's protocol (Illumina, San Diego, CA, USA). Sequencing was performed on the NovaSeq X Plus platform (Illumina, USA) with a paired-end 150 bp (PE150) read length.

Raw reads were trimmed and quality-controlled using fastp [18]. Clean reads were assembled de novo using Trinity [19]. Assembled transcripts were filtered using CD-HIT [20] and TransRate [21], and assembly completeness was assessed with BUSCO [22]. Functional annotation was performed by aligning transcripts against the NR, COG, and KEGG databases using Diamond (E-value $\leq 1.0 \times 10^{-5}$), and GO annotations were obtained using BLAST2GO (Version 2.9.0) [23]. Gene expression levels were quantified using RSEM [24]. Differential expression analysis was performed using DESeq2 [25], with $|\log_2 FC| \geq 1$ and FDR < 0.05 as the threshold for significantly differentially expressed genes. GO and KEGG enrichment analyses were conducted using Goatools and Python (Version1.0.0) scipy, respectively, with Bonferroni-corrected $p < 0.05$ considered significant. Bioinformatics analyses were performed on the Majorbio Cloud Platform (https://cloud.majorbio.com) (accessed on 15 May 2026).

2.6. Metabolomics Analysis

Liver samples (100 mg) from juvenile *R. ventralis* were extracted with 800 μL of methanol:water (4:1, *v*/*v*) containing 0.02 mg/mL L-2-chlorophenylalanine as an internal standard. The mixture was homogenized at −10 °C for 6 min, ultrasonicated at 5 °C for 30 min, and centrifuged at 13,000× *g* for 15 min at 4 °C. The supernatant was collected for LC-MS/MS analysis.

A pooled quality control (QC) sample was prepared by mixing equal volumes of all samples and injected every 5–10 runs to monitor system stability. LC-MS/MS analysis was performed on a UHPLC-Orbitrap Exploris 240 system equipped with an HSS T3 column (100 mm × 2.1 mm, 1.8 μm). The mobile phases consisted of 0.1% formic acid in water/acetonitrile (95:5, *v*/*v*) (A) and 0.1% formic acid in acetonitrile/isopropanol/water (47.5:47.5:5, *v*/*v*/*v*) (B). The flow rate was 0.40 mL/min, and the column temperature was 40 °C. Mass spectrometry was performed in positive and negative ion modes (*m*/*z* 70–1050). Raw data were processed using Progenesis QI. Metabolites were identified using the HMDB, Metlin, and Majorbio in-house databases. Data were analyzed on the Majorbio Cloud Platform (https://cloud.majorbio.com) (accessed on 15 May 2026). PCA and OPLS-DA

were performed using the R package (Version 1.6.2) "ropls". Metabolites with VIP > 1 and $p < 0.05$ were considered significantly different. KEGG pathway enrichment was performed using Fisher's exact test. All metabolomics data analyses were performed on majorbio choud platform.

2.7. Calculations and Statistical Analysis

Initial body weight (IBW), final body weight (FBW), weight gain (WG), specific growth rate (SGR), survival rate (SR), feed utilization efficiency (FUE), and hepatosomatic index (HSI) were calculated according to the following formulas:

$$\text{Weight gain (g)} = \text{Final body weight (g)} - \text{Initial body weight (g)}$$

$$\text{Specific growth rate (\%/day)} = [(\ln \text{final body weight} - \ln \text{initial body weight})/\text{rearing days (days)}] \times 100$$

$$\text{Survival rate (\%)} = (\text{Number of surviving individuals}/\text{Initial total number of individuals}) \times 100$$

$$\text{Hepatosomatic index (\%)} = (\text{Hepatopancreas weight (g)}/\text{Body weight (g)}) \times 100$$

$$\text{Feed utilization efficiency (\%)} = (\text{Weight gain (g)}/\text{Feed intake (g)}) \times 100$$

To evaluate the effects of different nutritional enhancers on the growth performance and antioxidant capacity of juvenile *R. ventralis*, one-way analysis of variance (ANOVA) was performed on survival rate, final body weight, weight gain, specific growth rate, feed utilization efficiency, hepatic SOD, CAT, and MDA concentration. Duncan's multiple range test was employed to analyze the significant differences among the COS group, CGA group, TH group, and CON group. All statistical analyses were conducted using SPSS software (version 24.0, SPSS Inc., Chicago, IL, USA), and the significance level was set at $p < 0.05$.

3. Results

3.1. Effects of Dietary Chitosan Oligosaccharide, Chlorogenic Acid, and Thymosin on Growth Performance

The growth performance of juvenile *R. ventralis* fed diets supplemented with COS, CGA, and TH is presented in Table 2.

Table 2. The effects of dietary chitosan oligosaccharide, chlorogenic acid, and thymosin on growth performance of *Rhinogobio ventralis*.

Parameters	Con	COS	CGA	TH
IBW (g)	1.02 ± 0.02	1.00 ± 0.02	1.05 ± 0.02	0.99 ± 0.02
FBW (g)	1.57 ± 0.20^{c}	2.12 ± 0.25^{a}	1.96 ± 0.22^{ab}	1.69 ± 0.21^{bc}
WGR (%)	54.02 ± 7.21^{d}	112.30 ± 12.45^{a}	86.95 ± 9.88^{b}	70.81 ± 8.32^{c}
SGR (%/day)	0.71 ± 0.09^{d}	1.24 ± 0.11^{a}	1.03 ± 0.10^{b}	0.89 ± 0.09^{c}
FCR	2.97 ± 0.17^{a}	1.34 ± 0.02^{d}	1.79 ± 0.04^{c}	2.60 ± 0.15^{b}
SR	100	100	100	100
CF (g/cm^3)	1.58 ± 0.12^{ab}	1.72 ± 0.15^{a}	1.66 ± 0.13^{ab}	1.55 ± 0.11^{b}

Different superscripts within rows indicate a significant difference between treatments ($p < 0.05$). Values are expressed as means ± standard deviations ($n = 3$).

All groups exhibited 100% survival throughout the experimental period. No significant differences were observed in initial body weight (IBW) among all groups ($p > 0.05$), indicating that the initial experimental conditions were comparable. In the following text, all descriptions of "no significant difference" indicate that the $p > 0.05$. Final body

weight (FBW), weight gain rate (WGR), and specific growth rate (SGR) were significantly affected by dietary supplementation ($p < 0.05$). Fish fed the COS diet exhibited the highest FBW (2.12 g), WGR (112.30%), and SGR (1.24%/day), followed by those fed the CGA diet (1.96 g, 86.95%, 1.03%/day). The control group (Con) showed the lowest values (1.57 g, 54.02%, 0.71%/day). Fish fed the TH diet displayed intermediate values (1.69 g, 70.81%, 0.89%/day). Feed conversion ratio (FCR) was also significantly influenced by dietary treatments ($p < 0.05$). The COS group exhibited the lowest FCR (1.34), which was significantly lower than that of the control group (2.97), followed by the CGA group (1.79) and the TH group (2.60). The control group showed the highest FCR, indicating the poorest feed efficiency. Condition factor (CF) ranged from 1.55 to 1.72 g/cm^3 across all groups. The COS group exhibited the highest CF (1.72), which was significantly higher than that of the TH group (1.55) ($p < 0.05$), but showed no significant differences from the control (1.58) or CGA (1.66) groups.

3.2. Effects of Dietary Chitosan Oligosaccharide, Chlorogenic Acid, and Thymosin on Hepatic Antioxidant Enzyme Activities

The effects of dietary supplementation with COS, CGA and TH on hepatic antioxidant enzyme activities of juvenile *R. ventralis* are presented in Table 3. Catalase (CAT) activity was significantly affected by dietary treatments ($p < 0.05$). The COS group exhibited the highest CAT activity (16.23 U/mg prot), which was significantly higher than that of all other groups ($p < 0.05$). No significant differences were observed between the CGA group (12.30 U/mg prot) and the TH group (12.17 U/mg prot), while the control group (13.11 U/mg prot) showed intermediate values. Superoxide dismutase (SOD) activity was also significantly influenced by dietary supplementation ($p < 0.05$).

Table 3. Effects of dietary chitosan oligosaccharide, chlorogenic acid and thymosin on hepatic antioxidant indices of *Rhinogobio ventralis*.

Item	Con	COS	CGA	TH
CAT/(U/mg prot)	13.11 ± 0.33 ^{b}	16.23 ± 0.17 ^{a}	12.30 ± 0.14 ^{c}	12.17 ± 0.33 ^{c}
SOD/(U/mg prot)	40.16 ± 2.41 ^{c}	45.41 ± 2.72 ^{a}	41.72 ± 2.50 ^{bc}	43.40 ± 2.60 ^{ab}
MDA/(nmol/mL)	4.46 ± 0.27 ^{a}	2.86 ± 0.17 ^{b}	4.11 ± 0.25 ^{a}	3.93 ± 0.24 ^{a}

Different superscripts within rows indicate a significant difference between treatments ($p < 0.05$). Values are expressed as means ± standard deviations ($n = 3$).

The COS group exhibited the highest SOD activity (45.41 U/mg prot), which was significantly higher than that of the control group (40.16 U/mg prot) ($p < 0.05$). The TH group (43.40 U/mg prot) showed no significant differences from the COS or CGA groups. The CGA group (41.72 U/mg prot) did not significantly differ from the control group. Malondialdehyde (MDA) content was significantly affected by dietary treatments ($p < 0.05$). The COS group exhibited the lowest MDA content (2.86 nmol/mL), which was significantly lower than that of all other groups ($p < 0.05$). No significant differences in MDA content were observed among the control group (4.46 nmol/mL), CGA group (4.11 nmol/mL), and TH group (3.93 nmol/mL).

3.3. Effects of Chitosan Oligosaccharide, Chlorogenic Acid, and Thymosin on the Liver Transcriptome

In this study, transcriptome sequencing was conducted on 16 juvenile *R. ventralis* individuals, yielding a total of 98.29 Gb of clean data, with no less than 5.54 Gb of clean data and a Q30 base percentage of ≥96.1% for each sample; de novo assembly using Trinity software (Version v2.8.5) yielded 101,366 transcripts and 67,746 non-redundant unigenes, with an N50 length of 2157 bp, and a total of 67,305 expressed unigenes detected. The Venn

diagram (Figure 1A) showed that 17,828 genes were co-expressed in all four groups, while principal component analysis (Figure 1B) revealed distinct differences in the transcriptional profiles among groups. The statistical analysis of differentially expressed genes is shown in Figure 1C. The volcano plots visually illustrated the distribution characteristics of DEGs in the three treatment groups. A total of 581 DEGs were identified in the COS vs. CON_G group, consisting of 163 up-regulated and 418 down-regulated genes (Figure 2A); 309 DEGs were detected in the CGA vs. CON_G group, including 77 up-regulated and 232 down-regulated genes (Figure 2B); and 293 DEGs were screened in the TH vs. CON_G group, with 59 up-regulated and 234 down-regulated genes (Figure 2C).

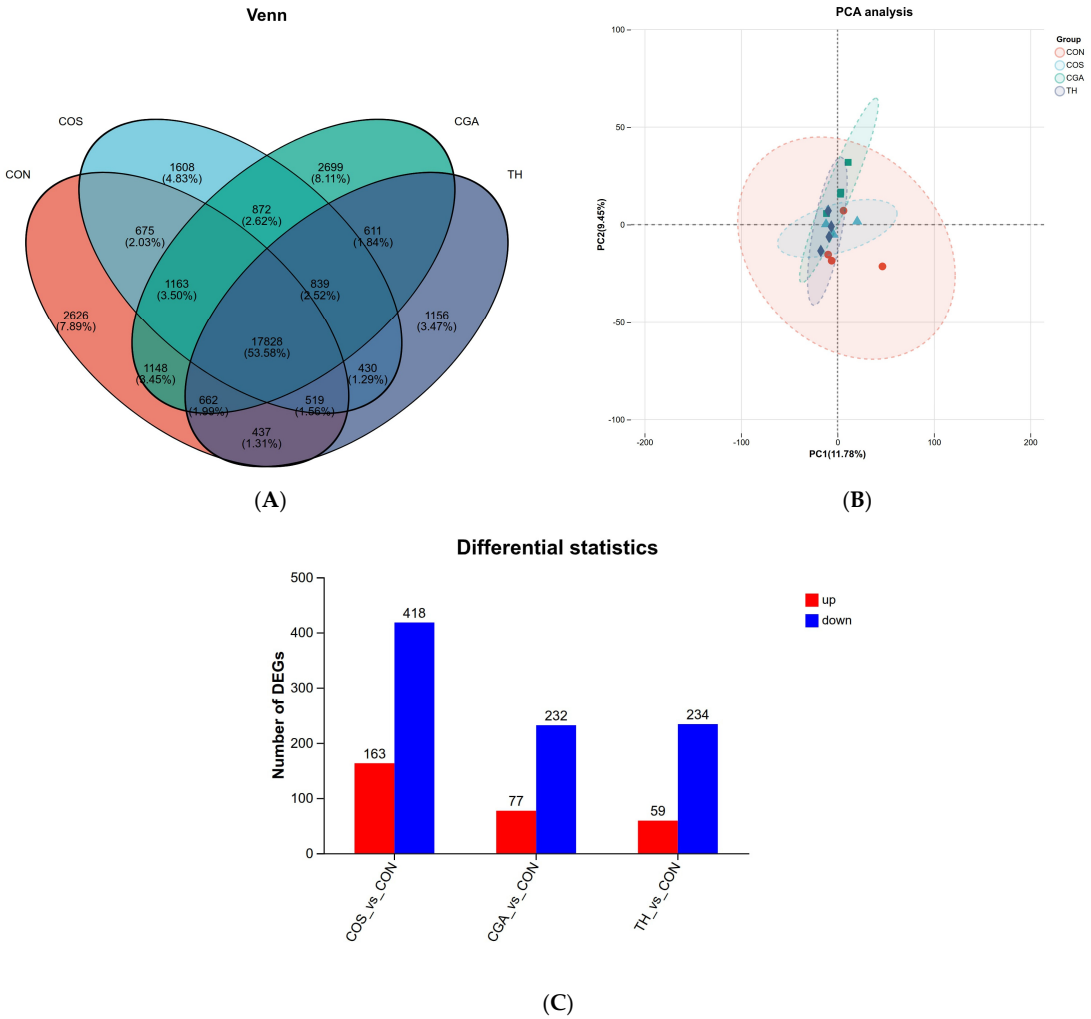

Figure 1. Transcriptomic and metabolomic analyses of *Rhinogobio ventralis* fed different experimental diets. (**A**) Venn diagram showing shared and unique differentially expressed genes and metabolites among groups. (**B**) PCA score plot of samples from different treatment groups. (**C**) Number of differentially expressed genes and metabolites in each treatment group compared with the control group.

KEGG pathway enrichment analysis is presented in Figure 3, where DEGs in the COS group (Figure 3A) were mainly enriched in signaling pathways such as PI3K-Akt, p53, FoxO, mTOR, and AMPK, as well as metabolic pathways including fatty acid biosynthesis and arginine biosynthesis, DEGs in the CGA group (Figure 3B) were significantly enriched in pathways including protein digestion and absorption, pancreatic secretion, gastric acid secretion, cAMP, FoxO, and AMPK signaling pathways, together with nicotinate and nicotinamide metabolism and fatty acid biosynthesis, DEGs in the TH group (Figure 3C)

were primarily enriched in signaling pathways including FoxO, p53, HIF-1, and PPAR, as well as nicotinate and nicotinamide metabolism, fatty acid biosynthesis, and ferroptosis, and pathways commonly enriched across all three treatment groups comprised the FoxO signaling pathway, fatty acid biosynthesis, and nicotinate and nicotinamide metabolism.

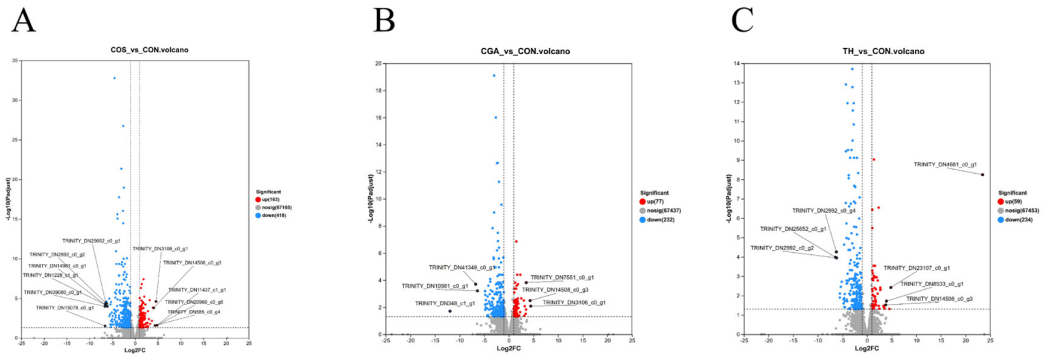

Figure 2. Volcano plots of differentially expressed genes in *Rhinogobio ventralis* between COS vs. CON groups (**A**), TH vs. CON groups (**B**), and CGA vs. CON groups (**C**).

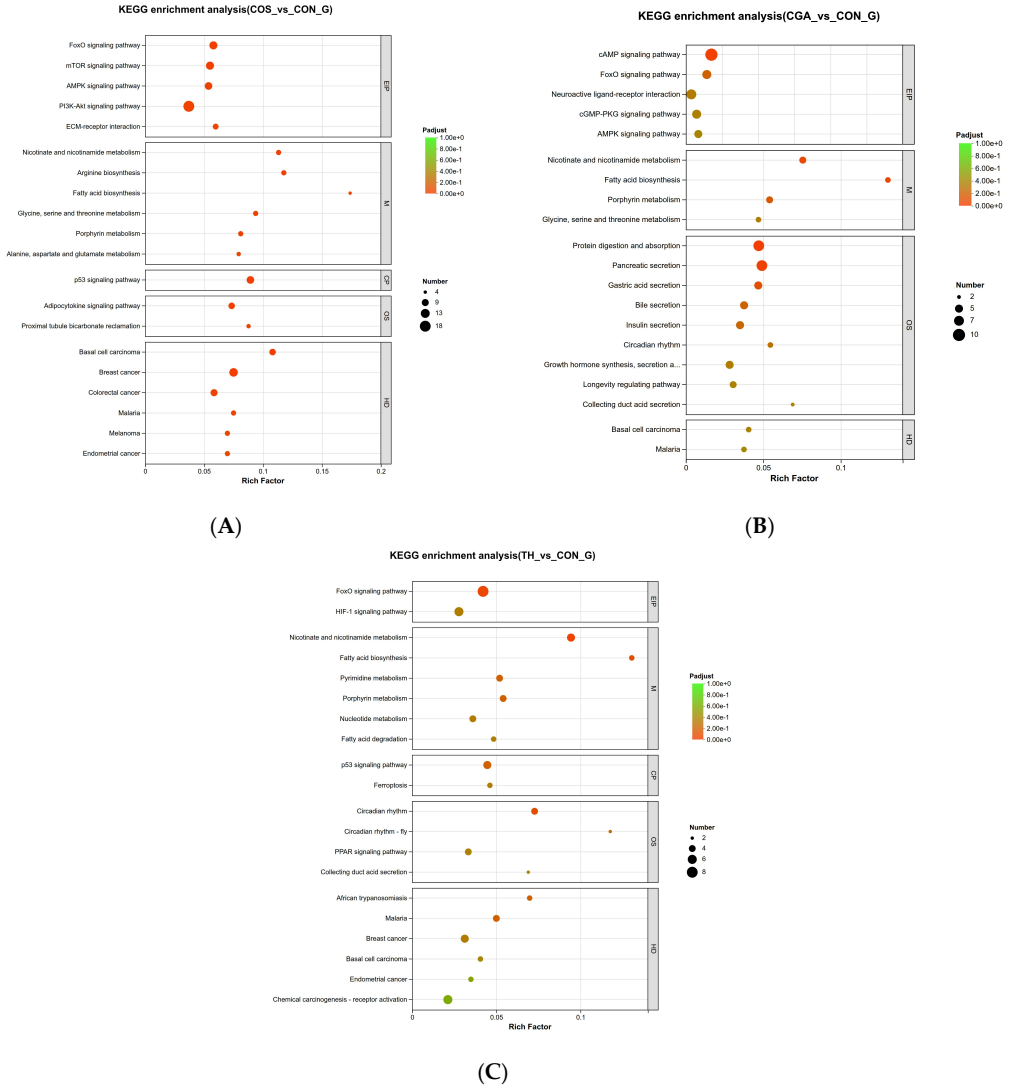

Figure 3. KEGG pathway enrichment analysis based on transcriptome of *Rhinogobio ventralis* fed COS vs. CON (**A**), CGA vs. CON (**B**), and TH vs. CON (**C**).

3.4. Effects of Chitosan Oligosaccharide, Chlorogenic Acid, and Thymosin on the Liver Metabolome

Non-targeted metabolomics analysis was performed on hepatopancreas samples of juvenile *R. ventralis* using liquid chromatography–mass spectrometry (LC-MS). The principal component analysis (PCA) score plot (Figure 4A) showed that PC1 explained 73.90% of the total variance and effectively distinguished the control group (CON) from the treatment groups (COS, CGA, TH). Samples in the CON group were clustered on the left side, while those in the COS, CGA and TH groups were concentrated on the right side, indicating that dietary supplementation with chitosan oligosaccharide, chlorogenic acid and thymopeptide significantly altered the metabolic profiles of juvenile *R. ventralis*. The Venn diagram (Figure 4B) showed that 3651 metabolites were shared by the four groups, accounting for 53.58% of the total metabolites; among them, there were 6 unique metabolites in the COS group, 8 in the CGA group and 3 in the TH group, suggesting a relatively stable metabolic background among groups.

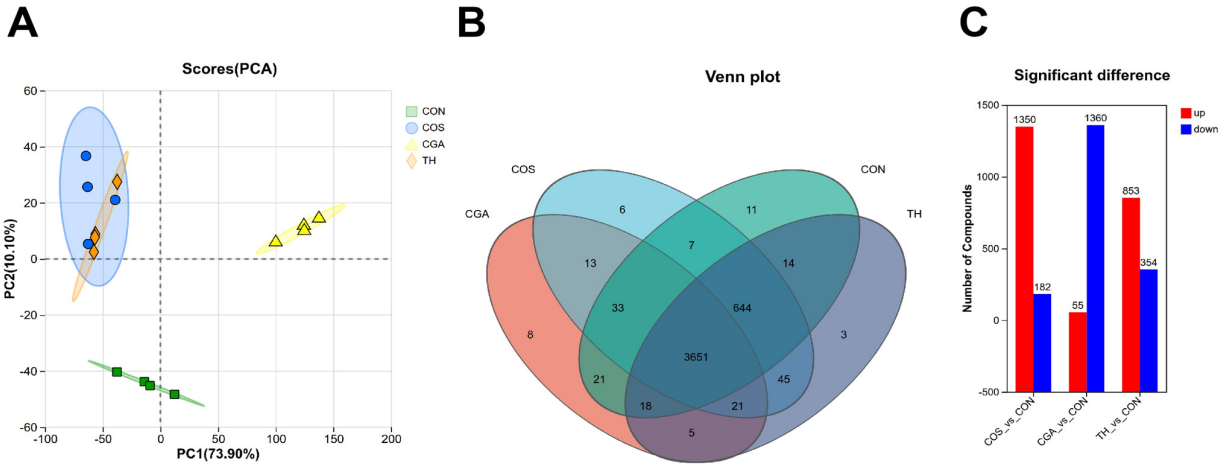

Figure 4. Metabolomic analysis of *Rhinogobio ventralis* fed different experimental diets. (**A**) PCA score plot; (**B**) Venn diagram of differentially expressed metabolites among groups; (**C**) Number of differentially expressed metabolites.

The results of differential metabolite analysis (Figure 4C) showed that compared with the CON group, 1532 differential metabolites (DEMs) were identified in the COS group, including 1350 upregulated and 182 downregulated metabolites; 1415 DEMs in the CGA group, with 55 upregulated and 1360 downregulated metabolites; and 1207 DEMs in the TH group, including 853 upregulated and 354 downregulated metabolites.

Volcano plot analysis of intergroup common differential metabolites (Figure 5A–C) further verified the distribution characteristics of DEMs in the three groups, with 1350 upregulated and 182 downregulated metabolites in the COS_vs_CON group, 55 upregulated and 1360 downregulated metabolites in the CGA_vs_CON group, and 853 upregulated and 354 downregulated metabolites in the TH_vs_CON group, which were completely consistent with the differential statistical results. Variable importance in projection (VIP) analysis (Figure 6A–C) screened the key DEMs with the highest contribution to grouping in each group. In the COS group, upregulated metabolites such as 3-O-feruloylquinic acid and phalloidin were the core biomarkers; in the CGA group, downregulated metabolites such as Pa(6-keto-PGF1α/16:0) and Leu-Asp-Glu-Lys were the core biomarkers; and in the TH group, bidirectionally regulated metabolites such as 3-O-feruloylquinic acid and panthenol were the core biomarkers.

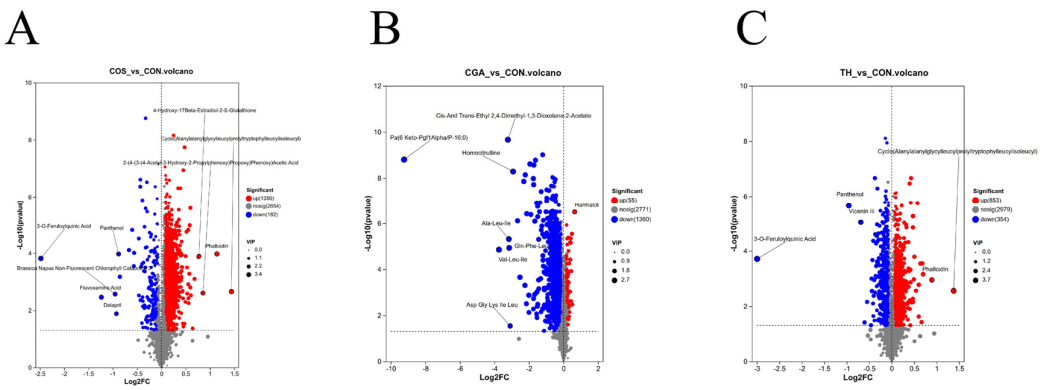

Figure 5. Volcano plots of differentially expressed metabolites in *Rhinogobio ventralis*. (**A**) COS vs. CON; (**B**) CGA vs. CON; (**C**) TH vs. CON. Red and blue points represent significantly upregulated and downregulated metabolites, respectively.

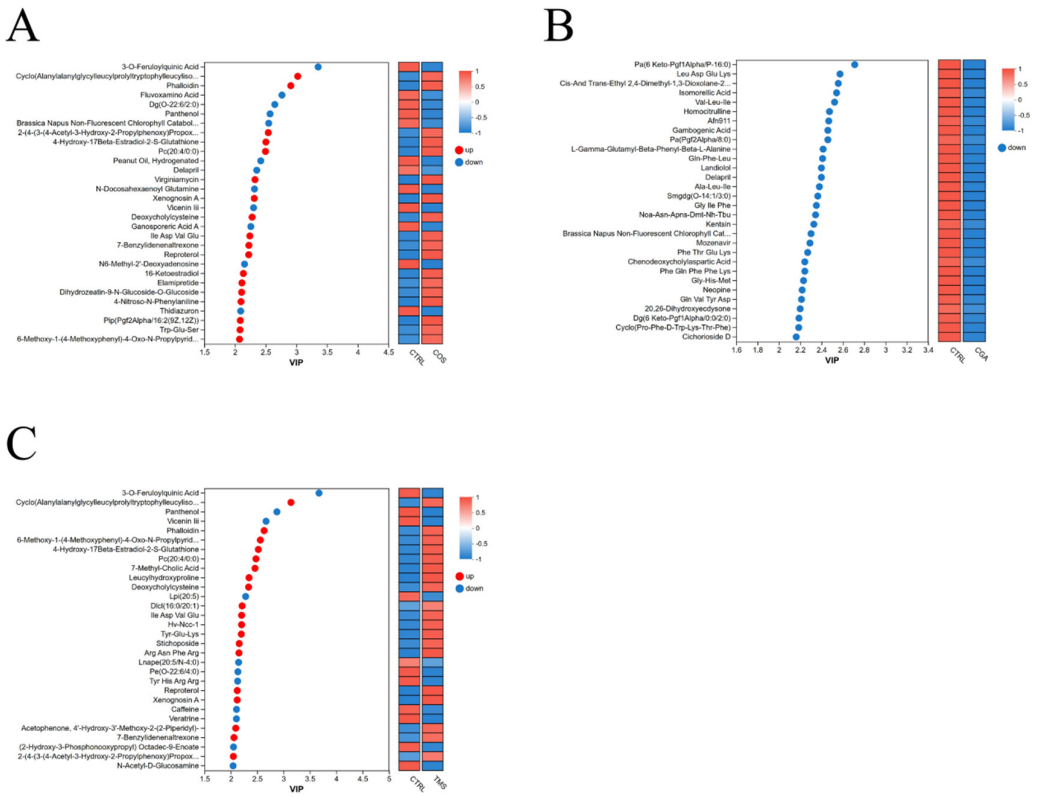

Figure 6. Variable importance in projection (VIP) of differentially expressed metabolites in *Rhinogobio ventralis* between the control and treatment groups (COS, CGA, TH). (**A**) COS vs. CON; (**B**) CGA vs. CON; (**C**) TH vs. CON.

KEGG pathway enrichment analysis was performed on the DEMs of the three groups, and the results are shown in Figure 6. Figure 7A (COS_vs_CON) showed that DEMs were mainly enriched in nucleotide metabolism, protein digestion and absorption, arachidonic acid metabolism, bile secretion, neuroactive ligand–receptor interaction, pyrimidine metabolism and other pathways. Figure 7B (CGA_vs_CON) showed that DEMs were significantly enriched in bile secretion, porphyrin metabolism, one-carbon pool by folate, neuroactive ligand–receptor interaction, FcεRI signaling pathway and other pathways. Figure 7C (TH_vs_CON) showed that DEMs were mainly enriched in neuroactive ligand–receptor interaction, central carbon metabolism in cancer, cGMP-PKG signaling pathway, nucleotide metabolism, porphyrin metabolism, bile secretion and other pathways. The

core pathways commonly enriched in all three groups included bile secretion, neuroactive ligand–receptor interaction and FcεRI signaling pathway.

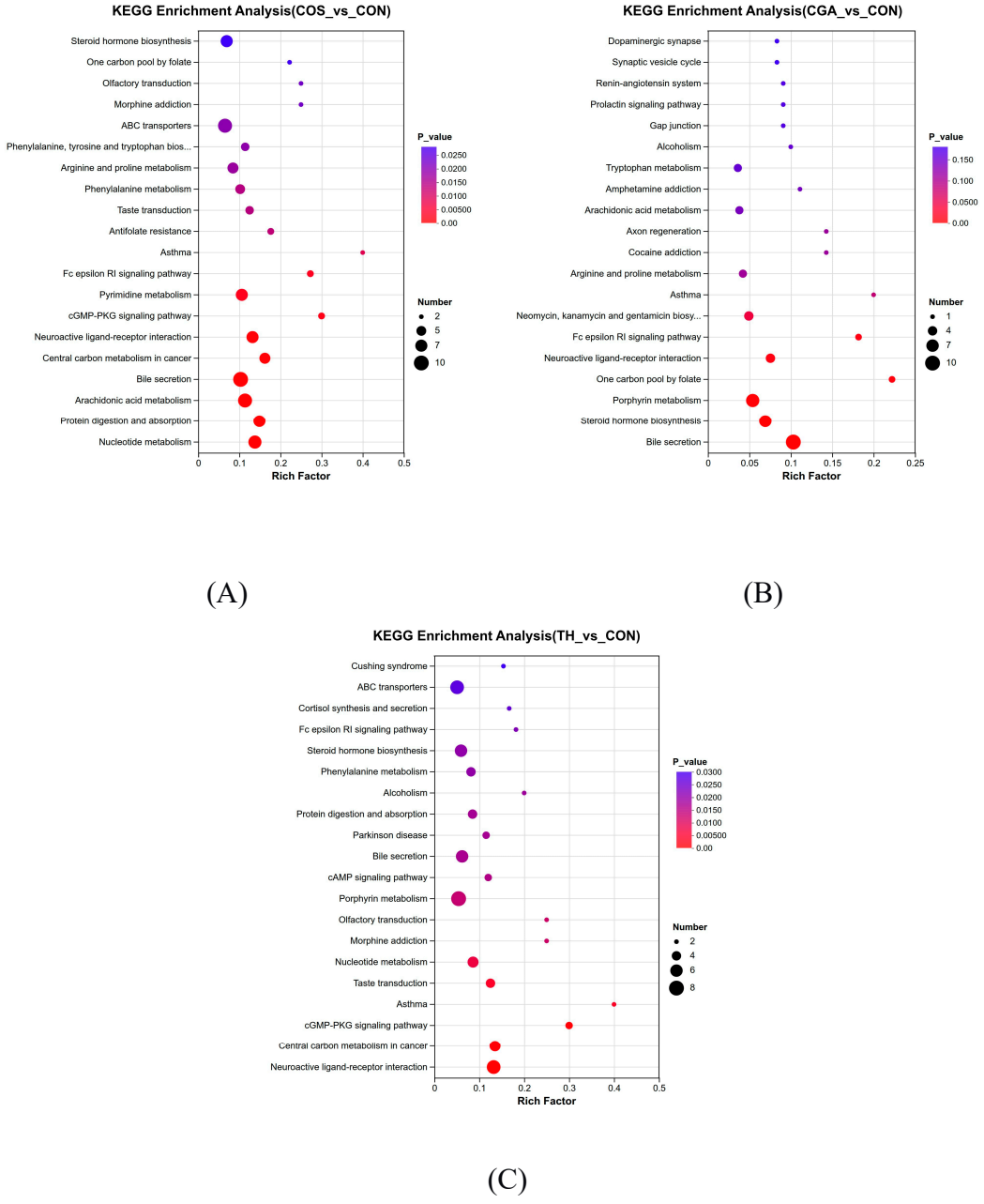

Figure 7. KEGG pathway enrichment analysis based on metabolome of *Rhinogobio ventralis* fed COS vs. CON (**A**), CGA vs. CON (**B**), and TH vs. CON (**C**).

3.5. Integration of Transcriptome and Metabolome Analyses in the Liver

An integrative analysis of KEGG pathways was performed, with the analysis being based on transcriptomic and metabolomic predictions. In the COS vs. CON group, the predictions of common KEGG pathways based on transcriptomic and metabolomic were "fat digestion and absorption", "linoleic acid metabolism", "arachidonic acid metabolism", "FoxO signaling pathway", "p53 signaling pathway", and "neuroactive ligand–receptor interaction" (Figure 8A). In the CGA vs. CON group, the predictions of common KEGG pathways based on transcriptomic and metabolomic analyses were "protein digestion and absorption", "Fc epsilon RI signaling pathway", "bile secretion", "fatty acid biosynthesis", "FoxO signaling pathway", "cAMP signaling pathway", and "neuroactive ligand–receptor

interaction" (Figure 8B). In the TH vs. CON group, the predictions of common KEGG pathways based on transcriptomic and metabolomic were "pyrimidine metabolism", "nucleotide metabolism", "fatty acid biosynthesis", "FoxO signaling pathway", "cAMP signaling pathway", "cGMP-PKG signaling pathway", "p53 signaling pathway", "neuroactive ligand–receptor interaction", and "central carbon metabolism in cancer" (Figure 8C). Of these, two KEGG pathways were shared across all three groups, namely "FoxO signaling pathway" and "neuroactive ligand–receptor interaction".

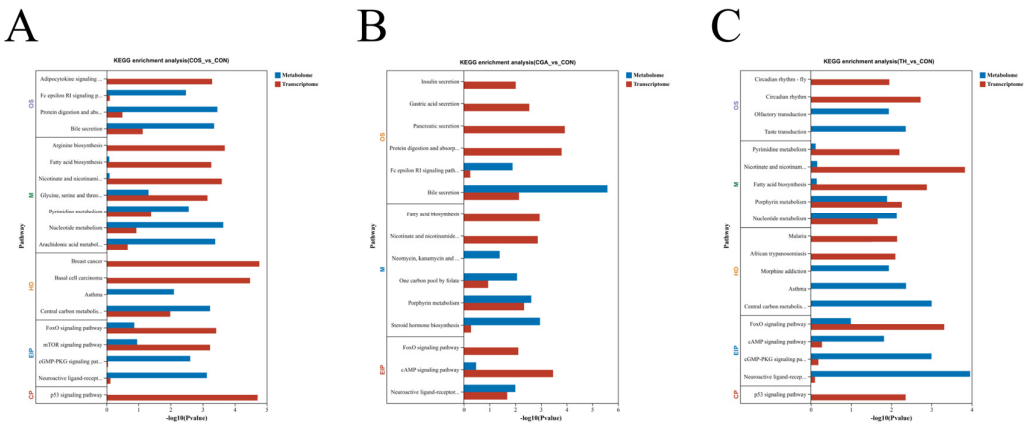

Figure 8. Integrated analysis of KEGG pathways based on transcriptome and metabolome of *Rhinogobio ventralis* fed COS vs. CON (**A**), CGA vs. CON (**B**), and TH vs. CON (**C**).

4. Discussion

In the field of aquatic animal nutrition, growth performance is recognized as a fundamental and critically important phenotypic indicator, which is routinely used to evaluate the effects of dietary components on the health and development of aquatic animals [26,27]. A number of studies have demonstrated that dietary supplementation with COS can significantly improve the growth performance of aquatic animals. Specifically, the addition of an appropriate amount of COS to the diet exerts significant effects on the WGR, SGR, FCR, and SR of *Litopenaeus vannamei* [28], *Cherax quadricarinatus* [29], and *O. niloticus* [8]. These findings are in agreement with the results obtained in this study. Similarly, relevant studies on *Oncorhynchus mykiss* [30], *Carassius carassius* [31], and grass carp [32] have also demonstrated that chlorogenic acid exerts significant effects on the growth performance of aquatic animals, which is consistent with the findings of the present study. Nevertheless, systematic and quantitative research regarding the effects of thymosin as a nutritional fortifier on fish growth performance has rarely been reported. The present study confirmed that dietary supplementation with chitosan oligosaccharide, chlorogenic acid and thymosin could significantly enhance the growth performance and feed utilization efficiency of juvenile *R. ventralis*. Among them, chitosan oligosaccharide exerted the most prominent growth-promoting effect, followed by chlorogenic acid, while thymosin exhibited a moderate improvement effect on growth.

In the liver, as the core organ for material metabolism and detoxification in aquatic animals, antioxidant capacity directly reflects the physiological state of the organism in scavenging Reactive Oxygen Species (ROS), alleviating oxidative stress, and resisting lipid peroxidation damage. It is also a key physiological index to evaluate the protective effect of feed additives on fish health [33]. As the first line of defense in the body's antioxidant defense system, SOD can specifically scavenge superoxide anion free radicals and reduce the initiation of oxidative damage; CAT mainly catalyzes the decomposition of hydrogen peroxide into water and oxygen, avoiding its accumulation in the body to cause lipid peroxidation [33,34]. MDA content, as the end product of lipid peroxidation, directly

reflects the degree of oxidative damage in the body. The lower the MDA content, the lighter the lipid peroxidation damage and the stronger the body's antioxidant capacity [35]. The present study revealed that dietary supplementation with COS significantly enhanced hepatic antioxidant enzyme activities, effectively eliminated reactive oxygen species, inhibited lipid peroxidation, and alleviated hepatic oxidative damage in *R. ventralis*. These findings are consistent with the report of Guan et al. [36], who demonstrated that chitosan oligosaccharides could improve antioxidant capacity and relieve oxidative stress in aquatic animals. The antioxidant regulation of COS is presumably attributed to its amino and hydroxyl structures, which can chelate metal ions, scavenge free radicals, or upregulate the expression of antioxidant-related genes, thereby activating the endogenous antioxidant defense system [7,37]. Furthermore, this antioxidant protection provides a critical mechanistic basis for the improved growth performance of *R. ventralis* fed COS-supplemented diets: reduced oxidative damage maintains normal hepatic metabolic function, promotes nutrient absorption and utilization, and ultimately optimizes growth parameters.

Compared with the COS group, the hepatic activities of antioxidant enzymes were slightly increased and the MDA content marginally decreased in the C and TH groups, with no significant differences from the control group, indicating mild regulatory effects of the two additives on the antioxidant system. As a natural plant polyphenol, chlorogenic acid has been confirmed to enhance the antioxidant capacity of aquatic animals by activating the Keap1/Nrf2 signaling pathway [10], while no significant regulatory effect was observed in the present study, which may be related to the dosage, experimental duration, or species specificity of *R. wilsoni*. Thymus peptides mainly act as immunostimulants focusing on regulating immune cell activity and enhancing antibacterial and antiviral abilities [12,38]. The weak modulation on the hepatic antioxidant system found in this study may be an indirect auxiliary way to improve health rather than the primary mechanism, which is consistent with previous reports that the antioxidant effect of thymosin is secondary, and its core function is immune regulation.

This study demonstrated that dietary COS, CGA, and TH significantly altered the liver transcriptomic and metabolomic profiles of *R. ventralis*. PCA clearly separated each treatment group from the control, indicating effective molecular regulation by all three additives. Notably, COS exhibited the strongest regulatory effects: 581 DEGs were identified in the COS group, which were 1.88-fold and 1.98-fold higher than those in the CGA (309) and TH (293) groups, respectively. At the metabolomic level, COS identified 1532 DEMs, representing 1.08-fold and 1.27-fold increases compared to CGA (1415) and TH (1207). These results suggest that COS induces broader transcriptional and metabolic reprogramming in the liver, consistent with its superior effects on growth performance and immune function. Similarly, chitosan oligosaccharide has been demonstrated to possess significant growth-promoting and immune-enhancing effects in *L. vannamei* [28] and *C. quadricarinatus* [29], with these effects being dose-dependent.

Mechanistically, COS uniquely activated a synergistic network of multiple signaling pathways, including PI3K-Akt, mTOR, AMPK, FoxO, and p53 [39]. The PI3K-Akt signaling pathway is a central regulator of cell survival, proliferation, and metabolism, and its activation has been linked to enhanced growth performance in fish [40]. The simultaneous enrichment of the PI3K-Akt-mTOR axis, which serves as a master regulator of cell growth, protein synthesis, and energy metabolism, likely underpins the superior growth-promoting effect of COS [41]. Furthermore, the co-activation of AMPK, an energy sensor, along with mTOR suggests that COS may coordinate anabolic and catabolic processes to maintain metabolic homeostasis while promoting growth [42]. The FoxO signaling pathway, which regulates oxidative stress resistance and apoptosis, was also enriched in the COS group, indicating that COS may enhance antioxidant capacity in addition to promoting growth [7,43].

The p53 pathway, another stress-responsive pathway, has been reported to play a role in cellular damage repair and immune regulation [44,45].

In contrast, both CGA and TH exhibited more restricted transcriptional signatures compared to COS. The CGA group lacked significant enrichment of the PI3K-Akt and mTOR pathways, which may explain its comparatively limited effect on growth performance [40,42]. Instead, CGA primarily affected pathways related to protein digestion and absorption, as well as the cAMP signaling pathway, suggesting a more focused role in nutrient utilization rather than broad-spectrum growth regulation. This is consistent with previous reports that chlorogenic acid improves antioxidant capacity and immune function in common carp and rainbow trout through the Keap-1/Nrf2 and NF-κB signaling pathways [10,30]. The cAMP signaling pathway, which was enriched in the CGA group, is known to mediate various physiological processes including immune responses and metabolic regulation [46]. The TH group exhibited the fewest DEGs among the three groups and uniquely enriched the ferroptosis pathway, along with HIF-1α and PPAR signaling pathways. Ferroptosis is a recently recognized form of regulated cell death characterized by iron-dependent lipid peroxidation, and its inhibition has been associated with tissue protection and anti-inflammatory effects [47]. The enrichment of the ferroptosis pathway in the TH group suggests that thymic peptide may protect hepatocytes from oxidative damage by suppressing ferroptotic cell death. This is consistent with previous studies demonstrating that thymosin β-4 participates in wound healing, tissue repair, and antibacterial immunity in black tiger shrimp and Hong Kong oyster [12,38]. The HIF-1α pathway mediates cellular adaptation to hypoxic and oxidative stress conditions [48], while the PPAR signaling pathway regulates lipid metabolism and inflammation [49].

KEGG pathway enrichment analysis of differential metabolites further highlighted the distinct metabolic strategies of the three additives. In the COS group, DEMs were mainly enriched in pathways such as nucleotide metabolism, protein digestion and absorption, arachidonic acid metabolism, bile secretion, neuroactive ligand–receptor interaction, and pyrimidine metabolism. The enrichment of arachidonic acid metabolism is particularly noteworthy, as its products (e.g., prostaglandins, leukotrienes) play critical roles in inflammation and immune regulation [50]. In the CGA group, DEMs were significantly enriched in bile secretion, porphyrin metabolism, one carbon pool by folate, neuroactive ligand–receptor interaction, and Fc epsilon RI signaling pathway. Porphyrin metabolism is involved in heme biosynthesis and oxygen transport, while folate-mediated one-carbon metabolism is critical for nucleotide synthesis and methylation reactions [51]. The downregulation of most metabolites in the CGA group may reflect a metabolic suppression mechanism that reduces oxidative burden, as has been observed with certain plant-derived polyphenols [27]. In the TH group, DEMs were mainly enriched in neuroactive ligand–receptor interaction, central carbon metabolism in cancer, cGMP-PKG signaling pathway, nucleotide metabolism, porphyrin metabolism, and bile secretion. The bidirectional regulatory pattern observed in the TH group may reflect its dual role in both promoting protective metabolites and suppressing potentially harmful ones. Overall, these metabolomic signatures demonstrate that COS promotes an anabolic metabolic state favorable for growth, CGA induces a suppressive metabolic profile, and TH exerts a balanced bidirectional modulation.

The integrative analysis of KEGG pathways based on both transcriptomic and metabolomic predictions provided critical insights into the convergent and divergent molecular mechanisms of the three additives. Notably, two KEGG pathways were commonly enriched across all three groups: the FoxO signaling pathway and neuroactive ligand–receptor interaction. The FoxO signaling pathway regulates oxidative stress resistance, apoptosis, and metabolism, and its common enrichment suggests that all three additives may enhance cellular stress resistance and metabolic adaptation [52]. The neuroactive

ligand–receptor interaction pathway mediates communication between the nervous and immune systems, implying that neuroendocrine-immune crosstalk may contribute to the additive-induced immunomodulation in *R. ventralis* [53].

Despite these commonalities, substantial differences existed in the integrated pathway profiles among the three groups. The COS group uniquely enriched pathways involved in lipid metabolism, including "fat digestion and absorption", "linoleic acid metabolism", and "arachidonic acid metabolism". The enrichment of these pathways in the COS group alone suggests that COS may exert additional benefits on energy supply and inflammatory balance, further supporting its superior immunomodulatory capacity [7]. The CGA group uniquely enriched the "Fc epsilon RI signaling pathway", which is associated with allergic responses and mast cell activation, suggesting that chlorogenic acid may modulate type I hypersensitivity reactions [54]. Additionally, the CGA group showed unique enrichment of "bile secretion" at the integrated level, consistent with its effects on lipid metabolism and nutrient absorption [55].

Notably, neither CGA nor TH showed significant enrichment of the PI3K-Akt-mTOR axis or the lipid metabolism pathways (fat digestion, linoleic acid metabolism, arachidonic acid metabolism) that were uniquely enriched in the COS group. This absence further explains the superior growth-promoting and immunomodulatory effects of COS compared to CGA and TH, which is consistent with previous findings in Nile tilapia and Pacific white shrimp [8,29]. Based on these observations, we propose that COS is the most effective among the three additives in promoting growth and enhancing immunity in *R. ventralis*, primarily through the synergistic activation of the PI3K-Akt-mTOR-AMPK-FoxO signaling network and the broad upregulation of anabolic and lipid metabolism pathways. In contrast, chlorogenic acid appears to exert a more restricted effect centered on nutrient absorption, cAMP signaling, and metabolic suppression, whereas thymic peptide may serve as a cytoprotective agent against oxidative stress and ferroptosis, with additional effects on nucleotide metabolism and the cGMP-PKG pathway. These mechanistic insights provide a molecular basis for the selective application of these functional additives in the aquaculture of *R. ventralis* and other endangered fish species.

5. Conclusions

An 8-week feeding trial was conducted to evaluate dietary COS, CGA and TH in juvenile *R. ventralis*. All three supplements significantly improved growth performance and feed efficiency, with COS showing the optimal growth-promoting effect. COS markedly enhanced hepatic CAT and SOD activities and decreased MDA content, whereas CGA and TH exerted no significant antioxidant effects. Transcriptomic and metabolomic analyses revealed distinct molecular responses: COS activated anabolic metabolism, CGA suppressed metabolism, and TH showed bidirectional regulation. Common enriched pathways included FoxO signaling, fatty acid biosynthesis, neuroactive ligand–receptor interaction, and bile secretion. Integrated multi-omics identified FoxO signaling and neuroactive ligand–receptor interaction as core regulatory pathways. COS is recommended as the most effective functional feed additive for growth and antioxidant protection in this endangered fish species.

Author Contributions: J.G. designed and supervised the experiments. W.C., Z.W., M.G. and L.L. carried out experiments. W.C. analyzed the data and wrote the manuscript. J.G. and X.C. revised the manuscript. All authors have read and agreed to the published version of the manuscript.

Funding: This study was supported by Hubei Key Laboratory of Three Gorges Project for Conservation of Fishes No. 2024004-ZHX.

Institutional Review Board Statement: This study was performed according to the Guide for the Care and Use of Laboratory Animals at Huazhong Agricultural University, Wuhan, China. All experimental protocols in this study were approved by the Animal Experimental Ethical Inspection of Laboratory Animal Center, Huazhong Agricultural University, Wuhan, China (Approval code: 202606150003). All efforts were made to minimize the suffering of the fish.

Data Availability Statement: Data will be made available on request.

Acknowledgments: The authors would like to express their sincere gratitude to Huazhong Agricultural University and China Three Gorges Corporation. We also thank the reviewers for their detailed and constructive comments on this manuscript.

Conflicts of Interest: Authors Lin Luo and Min Guan employed by the Chinese Sturgeon Research Institute of China Three Gorges Corporation. The remaining authors declare that the research was conducted in the absence of any commercial or financial relationships that could be construed as a potential conflict of interest.

References

1. Zhao, Y.; Wu, X.; Zheng, W.; Li, X.; Zhu, Y.; Zhu, T.; Li, X. Chromosome-level genome assembly and annotation of the *Rhinogobio ventralis*, an endangered endemic fish from the Yangtze River. *Sci. Data* **2026**, *13*, 615. [CrossRef] [PubMed]
2. Huang, K.; Wang, R.; Hu, G.; Zhou, W.; Li, W.; Zou, H.; Wang, G.; Li, M. Immune response of *Rhinogobio ventralis* to *Ichthyophthirius multifiliis* infection: Insights from histopathological and real-time gene expression analyses. *Fish Shellfish. Immunol.* **2024**, *153*, 109801. [CrossRef] [PubMed]
3. Zhao, Q.; Li, S.; Wang, S.; Zhao, Z.; Li, X.; Sun, H.; Wu, X.; Wang, Z.; Li, F. Response of *Rhinogobio ventralis* skin to *Ichthyophthirius multifiliis* infection: Pathological, transcriptomic and metabolomic analyses. *Fish Shellfish. Immunol.* **2025**, *167*, 110679. [CrossRef] [PubMed]
4. El Basuini, M.F. Immunomodulatory, antioxidant, and growth-promoting properties of *Avicennia marina* leaf extract on Nile tilapia. *Sci. Rep.* **2025**, *15*, 43948. [CrossRef] [PubMed]
5. Caruso, F.; Toschi, A.; García-Beltrán, J.M.; Cuesta, A.; Bonnici, C.; Piva, A.; Esteban, M.Á.; Grilli, E.; Shehata, A. Microencapsulated botanicals and organic acids improve immune status and growth in gilthead seabream (*Sparus aurata* L.). *Aquac. Nutr.* **2026**, *2026*, 4213038. [CrossRef] [PubMed]
6. Vicente-Gil, S.; Simón, R.; Nogales-Mérida, S.; Nuñez-Ortiz, N.; Fouz, B.; Serra, C.; Ordás, M.C.; Abós, B.; Herranz-Jusdado, J.G.; Morel, E.; et al. Bacillus subtilis supplemented feeding as a method to increase IgM titers and affinity in response to fish vaccination. *Fish Shellfish. Immunol.* **2025**, *162*, 110335. [CrossRef] [PubMed]
7. Mohan, K.; Rajan, D.K.; Ganesan, A.R.; Divya, D.; Johansen, J.; Zhang, S. Chitin, chitosan and chitooligosaccharides as potential growth promoters and immunostimulants in aquaculture: A comprehensive review. *Int. J. Biol. Macromol.* **2023**, *251*, 126285. [CrossRef] [PubMed]
8. Lu, C.L.; Wangkahart, E.; Huang, J.W.; Huang, Y.X.; Huang, Y.; Cai, J.; Jian, J.C.; Wang, B. Immune response and protective efficacy of *Streptococcus agalactiae* vaccine coated with chitosan oligosaccharide for different immunization strategy in Nile tilapia (*Oreochromis niloticus*). *Fish Shellfish. Immunol.* **2024**, *145*, 109353. [CrossRef] [PubMed]
9. Fu, H.; Qi, M.; Yang, Q.; Li, M.; Yao, G.; Bu, W.; Zheng, T.; Pi, X. Effects of dietary chito-oligosaccharide and β-glucan on the water quality and gut microbiota, intestinal morphology, immune response, and meat quality of Chinese soft-shell turtle (*Pelodiscus sinensis*). *Front. Immunol.* **2023**, *14*, 1266997. [CrossRef] [PubMed]
10. Shang, G.J.; Liu, S.Y.; Zhu, R.; Li, D.L.; Meng, S.T.; Wang, Y.T.; Wu, L.F. Chlorogenic acid improves common carp (*Cyprinus carpio*) liver and intestinal health through Keap-1/Nrf2 and NF-κB signaling pathways: Growth performance, immune response and antioxidant capacity. *Fish Shellfish. Immunol.* **2024**, *146*, 109378. [CrossRef] [PubMed]
11. Zhang, H.; Guo, H.; Lin, J.; He, X.; Rong, H.; Lin, F.; Wen, X. Dietary chlorogenic acid improved muscle quality, antioxidant capacity, and pro-inflammatory responses of blackspotted croaker *Protonibea diacanthus*. *Aquac. Nutr.* **2024**, *2024*, 7867796. [CrossRef] [PubMed]
12. Lin, C.; Qiu, L.; Wang, P.; Zhang, B.; Yan, L.; Zhao, C. Thymosin beta-4 participate in antibacterial immunity and wound healing in black tiger shrimp, *Penaeus monodon*. *Fish Shellfish. Immunol.* **2023**, *141*, 109065. [CrossRef] [PubMed]
13. Bai, L.; He, W.; Fan, S.; Liu, B.; Zhou, T.; Zhang, D.; Zhang, D.; Yu, D. Multiple functions of thymosin β4 in the pearl oyster *Pinctada fucata* suggest its multiple potential roles in artificial pearl culture. *Fish Shellfish. Immunol.* **2020**, *103*, 23–31. [CrossRef] [PubMed]

14. Núñez-Acuña, G.; Gonçalves, A.T.; Valenzuela-Muñoz, V.; Pino-Marambio, J.; Wadsworth, S.; Gallardo-Escárate, C. Transcriptome immunomodulation of in-feed additives in Atlantic salmon *Salmo salar* infested with sea lice *Caligus rogercresseyi*. *Fish Shellfish. Immunol.* **2015**, *47*, 450–460. [CrossRef] [PubMed]
15. Chen, D.; Lu, L.; Pei, Q.; Chen, D.; Yang, L.; Zhang, X.; Zhang, X.; Ouyang, P.; Geng, Y.; Li, Z.; et al. Transcriptome analysis of the immunomodulatory effects of *Salvia miltiorrhiza* polysaccharide on hemocyte immune response in *Procambarus clarkii*. *Fish Shellfish. Immunol.* **2022**, *131*, 697–706. [CrossRef] [PubMed]
16. Natnan, M.E.; Low, C.F.; Chong, C.M.; Bunawan, H.; Baharum, S.N. Oleic acid as potential immunostimulant in metabolism pathways of hybrid grouper fingerlings (*Epinephelus fuscoguttatus* × *Epinephelus lanceolatus*) infected with *Vibrio vulnificus*. *Sci. Rep.* **2023**, *13*, 12830. [CrossRef] [PubMed]
17. Jia, R.; Hou, Y.; Feng, W.; Nomingerel, M.; Li, B.; Zhu, J. Multi-omics analysis to understand the effects of dietary proanthocyanidins on antioxidant capacity, muscle nutrients, lipid metabolism, and intestinal microbiota in *Cyprinus carpio*. *Antioxidants* **2023**, *12*, 2095. [CrossRef] [PubMed]
18. Chen, S.; Zhou, Y.; Chen, Y.; Gu, J. fastp: An ultra-fast all-in-one FASTQ preprocessor. *Bioinformatics* **2018**, *34*, i884–i890. [CrossRef] [PubMed]
19. Grabherr, M.G.; Haas, B.J.; Yassour, M.; Levin, J.Z.; Thompson, D.A.; Amit, I.; Adiconis, X.; Fan, L.; Raychowdhury, R.; Zeng, Q.; et al. Full-length transcriptome assembly from RNA-Seq data without a reference genome. *Nat. Biotechnol.* **2011**, *29*, 644–652. [CrossRef] [PubMed]
20. Fu, L.; Niu, B.; Zhu, Z.; Wu, S.; Li, W. CD-HIT: Accelerated for clustering the next-generation sequencing data. *Bioinformatics* **2012**, *28*, 3150–3152. [CrossRef] [PubMed]
21. Smith-Unna, R.; Boursnell, C.; Patro, R.; Hibberd, J.M.; Kelly, S. TransRate: Reference-free quality assessment of *de novo* transcriptome assemblies. *Genome Res.* **2016**, *26*, 1134–1144. [CrossRef] [PubMed]
22. Manni, M.; Berkeley, M.R.; Seppey, M.; Simão, F.A.; Zdobnov, E.M. BUSCO update: Novel and streamlined workflows along with broader and deeper phylogenetic coverage for scoring of eukaryotic, prokaryotic, and viral genomes. *Mol. Biol. Evol.* **2021**, *38*, 4647–4654. [CrossRef] [PubMed]
23. Conesa, A.; Götz, S.; García-Gómez, J.M.; Terol, J.; Talón, M.; Robles, M. Blast2GO: A universal tool for annotation, visualization and analysis in functional genomics research. *Bioinformatics* **2005**, *21*, 3674–3676. [CrossRef] [PubMed]
24. Li, B.; Dewey, C.N. RSEM: Accurate transcript quantification from RNA-Seq data with or without a reference genome. *BMC Bioinform.* **2011**, *12*, 323. [CrossRef] [PubMed]
25. Love, M.I.; Huber, W.; Anders, S. Moderated estimation of fold change and dispersion for RNA-seq data with DESeq2. *Genome Biol.* **2014**, *15*, 550. [CrossRef] [PubMed]
26. Han, C.; Shi, C.; Liu, L.; Han, J.; Yang, Q.; Wang, Y.; Li, X.; Fu, W.; Gao, H.; Huang, H.; et al. Majorbio Cloud 2024: Update single-cell and multiomics workflows. *iMeta* **2024**, *3*, e217. [PubMed]
27. Kuebutornye, F.K.A.; Roy, K.; Folorunso, E.A.; Mraz, J. Plant-based feed additives in *Cyprinus carpio* aquaculture. *Rev. Aquac.* **2024**, *16*, 309–336. [CrossRef]
28. Liu, Y.; Xing, R.; Liu, S.; Qin, Y.; Li, K.; Yu, H.; Li, P. Effects of chitooligosaccharides supplementation with different dosages, molecular weights and degrees of deacetylation on growth performance, innate immunity and hepatopancreas morphology in Pacific white shrimp (*Litopenaeus vannamei*). *Carbohydr. Polym.* **2019**, *226*, 115254. [CrossRef] [PubMed]
29. Zhang, Z.L.; Cao, Y.L.; Xu, J.R.; Zhang, X.X.; Li, J.J.; Li, J.T.; Zheng, P.H.; Xian, J.A.; Lu, Y.P. Effects of dietary chitosan oligosaccharide on the growth, intestinal microbiota and immunity of juvenile red claw crayfish (*Cherax quadricarinatus*). *Fish Shellfish. Immunol.* **2024**, *145*, 109288. [CrossRef] [PubMed]
30. Ghafarifarsani, H.; Nedaei, S.; Hoseinifar, S.H.; Van Doan, H. Effect of different levels of chlorogenic acid on growth performance, immunological responses, antioxidant defense, and disease resistance of rainbow trout (*Oncorhynchus mykiss*) juveniles. *Aquac. Nutr.* **2023**, *2023*, 3679002. [CrossRef] [PubMed]
31. Jin, X.; Su, M.; Liang, Y.; Li, Y. Effects of chlorogenic acid on growth, metabolism, antioxidation, immunity, and intestinal flora of crucian carp (*Carassius auratus*). *Front. Microbiol.* **2023**, *13*, 1084500. [CrossRef] [PubMed]
32. Yang, H.; Xu, Z.; Li, X.; Leng, X. Individual and combined effects of dietary chlorogenic acid and quercetin supplementation on the growth, lipid metabolism and flesh quality of grass carp, *Ctenopharyngodon idellus*. *Anim. Feed. Sci. Technol.* **2024**, *318*, 116129. [CrossRef]
33. Moezzi, S.A.; Ramezani, S.; Rezaei, K.; Khoei, A.J. Mechanisms of pesticide toxicity in fish: Insights into the ameliorative role of plant-derived compounds—A review. *Aqua. Nutr.* **2025**, *2025*, 5328773. [CrossRef] [PubMed]
34. Zeng, Y.; Song, Z.; Song, G.; Li, S.; Sun, H.; Zhang, C.; Li, G. Oxidative stress and antioxidant biomarker responses in fish exposed to heavy metals: A review. *Environ. Monit. Assess.* **2025**, *197*, 892. [CrossRef] [PubMed]
35. Chen, G.; Xu, C.; Wang, Z.; Han, Z.; Xia, Q.; Wei, S.; Sun, Q.; Liu, S. Effect of MDA-mediated oxidation on the protein structure and digestive properties of golden pomfret. *Food Chem.* **2024**, *443*, 138563. [CrossRef] [PubMed]

36. Guan, D.; Sun, H.; Meng, X.; Wang, J.; Wan, W.; Han, H.; Wang, Z.; Li, Y. Effects of different molar mass chitooligosaccharides on growth, antioxidant capacity, non-specific immune response, and resistance to *Aeromonas hydrophila* in GIFT tilapia *Oreochromis niloticus*. *Fish Shellfish. Immunol.* **2019**, *93*, 500–507. [CrossRef] [PubMed]
37. Basawa, R.; Kabra, S.; Khile, D.A.; Faruk Abbu, R.U.; Parekkadan, S.J.; Thomas, N.A.; Kim, S.K.; Raval, R. Repurposing chitin-rich seafood waste for warm-water fish farming. *Heliyon* **2023**, *9*, e18197. [CrossRef] [PubMed]
38. Li, J.; Zhang, Y.; Liu, Y.; Zhang, Y.; Xiang, Z.; Qu, F.; Yu, Z. A thymosin beta-4 is involved in production of hemocytes and immune defense of Hong Kong oyster, *Crassostrea hongkongensis*. *Dev. Comp. Immunol.* **2016**, *57*, 1–9. [CrossRef] [PubMed]
39. Pan, Z.; Cheng, D.; Wei, X.; Li, S.; Guo, H.; Yang, Q. Chitooligosaccharides inhibit tumor progression and induce autophagy through the activation of the p53/mTOR pathway in osteosarcoma. *Carbohydr. Polym.* **2021**, *258*, 117596. [CrossRef] [PubMed]
40. Huang, J.; Shi, C.; Gao, Y.; Su, J.; Shu, Y.; Zeng, N.; Zhai, G.; Jin, X.; Han, D.; He, J.; et al. Heterozygous depletion of pik3r1 improves growth and feed conversion efficiency in Gibel carp (*Carassius gibelio*). *Aquaculture* **2021**, *545*, 737207. [CrossRef]
41. Kumar, R.; Huang, J.Y.; Ng, Y.S.; Chen, C.Y.; Wang, H.C. The regulation of shrimp metabolism by the white spot syndrome virus (WSSV). *Rev. Aquac.* **2022**, *14*, 1150–1169. [CrossRef]
42. Wang, D.; Tian, Y.; Wang, Q.; Zhang, Y.; Ye, B.; Zuo, Z.; He, J.; Pan, Z.; Sun, D.; Zou, J.; et al. Cold stress-induced autophagy and apoptosis disorders are mainly mediated by AMPK/PPAR/PI3K/AKT/mTOR pathways. *Aquaculture* **2024**, *583*, 740574. [CrossRef]
43. Wang, X.; Chen, L.; Peng, J.; Luo, Z.; Zhang, M.; Ruan, G.; Zhao, X.; Zhang, Y.; Guo, Z.; Li, S. Apoptosis and FoxO signaling axis form the core antiviral defense in mud crab (*Scylla paramamosain*) against MCRV. *Aquaculture* **2026**, *617*, 743768. [CrossRef]
44. Tu, Z.; Tang, L.; Shen, H.; Hu, M.; Chen, F.; Wang, X.; Abo-Raya, M.H.; Wang, Y. Molecular insights into the physiological impact of low-frequency noise on sea slug *Onchidium reevesii*: Activation of p53 signaling and oxidative stress response. *J. Environ. Manag.* **2024**, *373*, 123481. [CrossRef] [PubMed]
45. Cheng, C.H.; Luo, S.W.; Ye, C.X.; Wang, A.L.; Guo, Z.X. Identification, characterization and expression analysis of tumor suppressor protein p53 from pufferfish (*Takifugu obscurus*) after the *Vibrio alginolyticus* challenge. *Fish Shellfish. Immunol.* **2016**, *59*, 312–322. [CrossRef] [PubMed]
46. Wu, C.; Li, Q.; Zhao, Z.; Sui, C.; Liu, Q.; Lai, W.; Zhang, J.; Li, Y.; Mai, K.; Ai, Q. FFAR4 functions as a DHA receptor to attenuate LPS-induced inflammation via the cAMP/IκBα pathway in large yellow croaker (*Larimichthys crocea*). *FASEB J.* **2025**, *39*, e71068. [CrossRef] [PubMed]
47. Gao, F.; Shi, X.; Pei, C.; Zhao, X.; Zhu, L.; Zhang, J.; Li, L.; Li, C.; Kong, X. The role of ferroptosis in fish inflammation. *Rev. Aquac.* **2023**, *15*, 318–332. [CrossRef]
48. Xiao, W. The hypoxia signaling pathway and hypoxic adaptation in fishes. *Sci. China Life Sci.* **2015**, *58*, 148–155. [CrossRef] [PubMed]
49. Dai, Y.F.; Lv, Z.M.; You, M.X.; Sun, L.L.; Li, C.H. PPARα alleviates inflammation via inhibiting NF-κB/Rel pathway in Vibrio splendidus challenged *Apostichopus japonicus*. *Fish Shellfish. Immunol.* **2023**, *138*, 108701. [CrossRef] [PubMed]
50. Yang, B.; Li, S.; Wang, S.; Jiang, D.; Yu, X.; Li, C.; Wu, X.; Xu, S.; Zhang, Y.; Yang, Q. High dietary arachidonic acid produces excess eicosanoids, and induces hepatic inflammatory responses, oxidative stress and apoptosis in juvenile *Acanthopagrus schlegelii*. *Aquac. Rep.* **2023**, *29*, 101506. [CrossRef]
51. Espe, M.; Adam, A.C.; Saito, T.; Whatmore, P.; Fernandes, J.M.O.; Vikeså, V.; Skjærven, K.H. Metabolic and molecular signatures of improved growth in Atlantic salmon (*Salmo salar*) fed surplus levels of methionine, folic acid, vitamin B_6 and B_{12} throughout smoltification. *Br. J. Nutr.* **2022**, *127*, 1289–1302. [CrossRef] [PubMed]
52. Chen, J.; Chen, D.; Li, J.; Liu, Y.; Gu, X.; Teng, X. Cadmium-induced oxidative stress and immunosuppression mediated mitochondrial apoptosis via JNK-FoxO3a-PUMA pathway in common carp (*Cyprinus carpio* L.) gills. *Aquat. Toxicol.* **2021**, *233*, 105775. [CrossRef] [PubMed]
53. García-Beltrán, J.M.; Johnstone, C.; Arizcun, M.; Cuesta, A.; Pérez, M.; Chaves-Pozo, E. The susceptibility of shi drum juveniles to betanodavirus increases with rearing densities in a process mediated by neuroactive ligand-receptor interaction. *Front. Immunol.* **2024**, *15*, 1304603. [CrossRef] [PubMed]
54. Sakurai, D.; Yamasaki, S.; Arase, K.; Park, S.Y.; Arase, H.; Konno, A.; Saito, T. Fc epsilon RI gamma-ITAM is differentially required for mast cell function in vivo. *J. Immunol.* **2004**, *172*, 2374–2381. [CrossRef] [PubMed]
55. Zhao, W.; Yao, R.; Wei, H.L.; Guo, Y.C.; Chen, A.Q.; Chen, B.Y.; Niu, J. Astaxanthin, bile acid and chlorogenic acid attenuated the negative effects of high-fat diet on the growth, lipid deposition, and liver health of *Oncorhynchus mykiss*. *Aquaculture* **2023**, *567*, 739255. [CrossRef]